Clin Neuroradiol (2019) 29:479–491
https://doi.org/10.1007/s00062-018-0676-2

ORIGINAL ARTICLE

In Vivo Molecular Profiling of Human Glioma

Cross-Sectional Observational Study Using Dynamic Susceptibility Contrast Magnetic Resonance Perfusion Imaging

Johann-Martin Hempel[1] · Jens Schittenhelm[2] · Uwe Klose[1] · Benjamin Bender[1] · Georg Bier[1] · Marco Skardelly[3] · Ghazaleh Tabatabai[4] · Salvador Castaneda Vega[5] · Ulrike Ernemann[1] · Cornelia Brendle[1]

Received: 18 September 2017 / Accepted: 2 February 2018 / Published online: 21 February 2018

Abstract

Purpose To assess the diagnostic performance of dynamic susceptibility contrast perfusion magnetic resonance perfusion imaging (DSC-MRI) for in vivo human glioma molecular profiling.

Methods In this study 100 patients with histopathologically confirmed glioma who provided written informed consent were retrospectively assessed between January 2016 and February 2017 in two prospective trials that were approved by the local institutional review board. Cerebral blood volume (CBV) measurements from DSC-MRI were assessed, and histogram parameters of relative CBV (rCBV) results were compared among World Health Organization (WHO) 2016 based histological findings and molecular characteristics. A classification and regression tree (CART) algorithm with 10-fold cross-validation was used to calculate the diagnostic accuracy.

Results The 90th percentile (C90) of rCBV was significantly lower in patients with the isocitrate dehydrogenase 1/2 (IDH1/2) mutation (2.86 ± 1.21; $p < 0.001$) and loss of alpha-thalassemia mental retardation syndrome X-linked (ATRX) expression (2.23 ± 0.91; $p < 0.001$) than in those with the IDH1/2 wild type (4.78 ± 2.34) and maintained ATRX expression (4.30 ± 2.02). The standard deviation (SD) of rCBV was significantly higher in glioblastoma (GBM) with methylated O6-methylguanine DNA methyltransferase (MGMT; 1.99 ± 0.73; $p = 0.001$) than in those with unmethylated MGMT (1.20 ± 0.45). In CART analysis, rCBV predicted the molecular subgroup in 76.3% of astroglial tumors; however, the diagnostic performance was reduced to 48.1% by including oligodendrogliomas with chromosome 1p/19q co-deletion in the analysis due to substantial overlap of rCBV values between $OD_{1p/19q\text{-}LOH}$ and IDH_{wt} GBM.

Conclusion The DSC-MRI procedure may provide insight into the IDH1/2 mutation and ATRX expression status and MGMT methylation profile of diffuse glioma; however, taking integrated oligodendroglioma into account limits the diagnostic performance of rCBV in non-invasively predicting the molecular subtype.

Keywords Glioma · Neoplasm grading · Perfusion imaging · Cerebral blood volume · Isocitrate dehydrogenase

Introduction

The recently updated World Health Organization classification (revised 4th edition) of tumors of the central nervous system (2016 CNS WHO) combines both histopathological and molecular features into an integrated diagnosis [1]. The molecular stratification is essential for estimating the individual prognosis [2, 3]. The relevant molecular characteristics are isocitrate dehydrogenase (IDH) 1/2 mutation status and chromosome 1p/19q loss of heterozygosity (LOH). They are complemented by alpha-thalassemia/mental retardation syndrome X-linked (ATRX), which again is predictive for associated IDH or H3F3A hotspot mutations [4]. The ATRX status itself confers a prognostic potential in diffuse gliomas [5]. The loss of ATRX expression is mostly induced by truncating ATRX mutations, resulting in an alternative lengthening of telomeres (ALT) phenotype [6, 7]. Also, O6-methylguanine DNA methyltransferase (MGMT)

Electronic supplementary material The online version of this article (https://doi.org/10.1007/s00062-018-0676-2) contains supplementary material, which is available to authorized users.

✉ Johann-Martin Hempel
johann-martin.hempel@uni-tuebingen.de

Extended author information available on the last page of the article

can be regarded as an independent prognostic factor in diffuse glioma [7–9].

Dynamic susceptibility-weighted magnetic resonance perfusion imaging (DSC-MRI) is an established imaging method that allows estimation of tumor tissue perfusion based on the loss of signal in T2*-weighted images after contrast agent bolus administration [10]. Cerebral blood volume (CBV) results from DSC-MRI reflect the vascular proliferation in tumors [11, 12] and has been shown to correlate with the WHO 2007-based histology and tumor grade [11, 13, 14]; however, several studies have shown discrepant results and there is substantial overlap for CBV-based tumor grading based on previous 2007 WHO classification [15–17]. In the context of the integrated diagnostic approach of the 2016 CNS WHO [1], normalized relative CBV (rCBV) has shown potential for differentiating between IDH-mutant and IDH wild type astrocytomas [18, 19]; however, its value has not yet been sufficiently investigated in the context of molecular stratification according to the newly launched integrated approach of 2016 CNS WHO. Therefore, this study aimed to assess the diagnostic performance of DSC-MRI for stratifying glioma according to the relevant prognostic molecular characteristics including IDH1/2 mutation, ATRX expression, chromosome 1p/19q LOH, and MGMT promoter methylation.

Material and Methods

Study Design and Ethics

The study was a retrospective cross-sectional analysis of prospective data acquired in two single-center, non-randomized trials, which were approved by the local institutional review board at our university hospital. The trials were conducted based on the principles of the International Conference on Harmonization: Good Clinical Practice guidelines, and according to the 2013 revised version of the Declaration of Helsinki. All patients provided written informed consent for the imaging surveys and subsequent use of clinical data for research and scientific purposes.

Patient Selection and Stratification

The study group was selected from 145 consecutive patients comprising 76 males and 69 females with a mean age of 50.4 ± 14.7 years (range, 20–81 years). Fig. 1 demonstrates the patient selection and dichotomization in a flow diagram and includes all inclusion and exclusion criteria. All studies were completed within 2 weeks of diagnosis and before initiating treatment. None of the patients received steroid treatment at the time of imaging. The final study group included 100 patients with a mean age of 51.4 ± 15.2 years

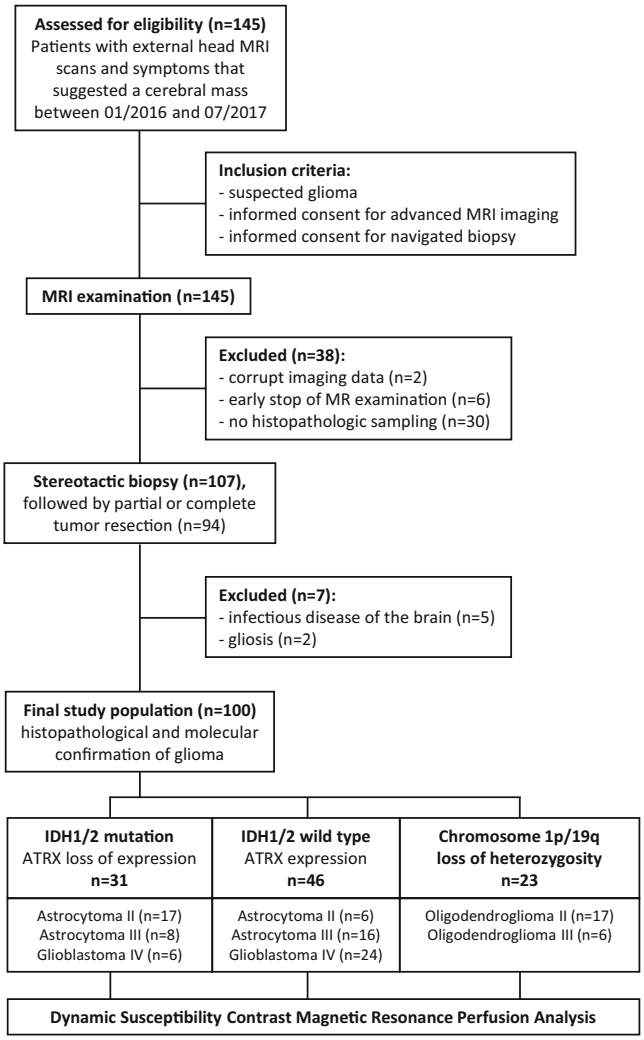

Fig. 1 Patient flow diagram

and comprised 55 men (55%) and 45 women (45%). The final diagnosis was based on histological examinations of specimens obtained by navigated biopsy in all patients followed by partial or complete tumor resection in 94 patients (94%).

The IDH mutation status was assessed by immunohistochemistry with a mutation-specific IDH1 R132H antibody [20, 21]. This was followed by Sanger sequencing of the negative samples to detect any non-canonical IDH1/2 mutations [22]. Nuclear ATRX status in tumor cells was determined by immunohistochemistry as described previously [4]. A synthetic high-resolution microsatellite PCR gel was used to study chromosome 1p/19q LOH in all tumors with an oligodendroglial component [23]. The MGMT status was assessed using methylation-specific PCR in all high-grade tumors [7, 24].

The tumors were classified according to the current 2016 CNS WHO criteria [2]. The combination of ATRX loss of expression and IDH1/2 mutation in the integrated

approach characterizes diffuse astrocytoma including its most aggressive histological subtype: secondary glioblastoma (GBM). Primary glioblastomas (GBMs) are tumors with IDH1/2 wild type and maintained ATRX expression. All gliomas with 1p/19q LOH and IDH1/2 mutation are considered to be oligodendrogliomas, and an overwhelming majority are associated with maintained ATRX expression [1, 25]. Additionally, IDH-mutant (IDH_{mut}) diffuse astrocytoma (AS2), IDH_{mut} anaplastic astrocytoma (AS3), and IDH_{mut} AS4/GBM were grouped as IDH_{mut} astrocytoma (AS); IDH wild type (IDH_{wt}) AS2, IDH_{wt} AS3, and IDH_{wt} AS4/GBM were grouped as IDH_{wt} GBM; and 1p/19q-confirmed diffuse (OD2) and anaplastic oligodendroglioma (OD3) were grouped as 1p/19q-confirmed oligodendroglioma ($OD_{1p/19q\text{-}LOH}$), based on their molecular profile and clinical outcome [2, 3, 5, 26].

Procedures and Techniques

Magnetic Resonance Imaging

Imaging was performed using a 3.0 T MRI scanner (Biograph mMR, Siemens Healthcare, Erlangen, Germany). The conventional MRI examination protocol included a transversal 2D-encoded T2-weighted fluid attenuated inversion recovery (FLAIR) sequence (TR/TE, 9000/87 ms; inversion time (TI), 2500 ms; slice thickness, 3 mm) and a sagittal 3D-encoded magnetization prepared rapid acquisition gradient echo (MPRAGE) sequence (TR/TE, 1900/2.4 ms; TI, 900 ms) before and after contrast agent administration (0.1 ml/kg body weight gadobutrol; Gadovist®, Bayer Healthcare, Leverkusen, Germany). After preloading with 2 × 0.1 mmol/kg gadobutrol at an injection rate of 3 ml/s to perform dynamic contrast-enhanced MRI, the dynamic susceptibility-weighted T2* sequence was performed during the first pass of contrast agent bolus (single-shot echo-planar imaging sequence, TR 1130 ms; TE, 31 ms; slice thickness, 4 mm; matrix size, 128 × 128; FoV, 230 × 230 mm^2). Fig. 2 shows a representative slice of CBV perfusion maps and anatomic FLAIR and contrast-enhanced MPRAGE images in a 56-year-old patient with histopathologically confirmed IDH_{wt} GBM who had maintained ATRX expression and a methylated MGMT promoter in the right frontal lobe.

Observer Setting

The CBV image analyses were performed independently by two board-certified physicians who were blinded to the clinical diagnoses: reader one had 8 years of experience and reader two had 7 years of experience in neuroradiological imaging. The intra-class correlation coefficient (ICC) was calculated for testing inter-observer agreement (0.00–0.20 poor, 0.21–0.40 fair, 0.41–0.60 moderate, 0.61–0.80 good, and 0.81–1.00 excellent correlation).

Image Post-processing

The DSC-MRI-based parametric perfusion maps were calculated, and leakage correction was performed using syngo® perfusion® (Siemens Healthcare). The medial or anterior cerebral artery was identified manually for the arterial input function. Image and volume of interest (VOI) analyses were performed using MIPAV 7.4.0 (http://mipav.cit.nih.gov/) and in-house Matlab®-based software (Matlab 2014b, MathWorks Natick, MA, USA). The VOIs were manually drawn on the anatomic transverse FLAIR-weighted images around the most solid-appearing parts of

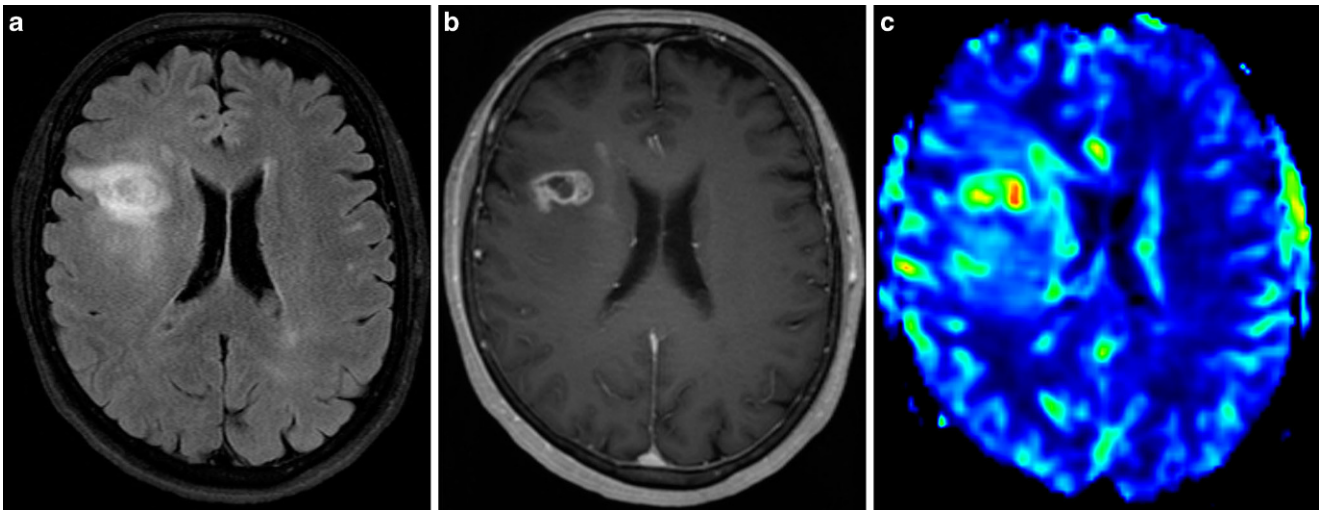

Fig. 2 FLAIR (**a**), contrast enhancement axial reformatted T1 MPRAGE (**b**), and DSC-rCBV perfusion maps (**c**) in a 56-year-old patient with histopathologically confirmed IDH wild type glioblastoma WHO grade IV, maintained ATRX expression, and methylated MGMT promoter

each whole tumor on multiple slices, indicated by T2 signal alterations, as well as in the contralateral frontoparietal supraventricular normal-appearing white matter (NAWM). By encompassing the whole tumor, we sought to minimize potential sampling bias [27]. The CBV parametric maps were then transformed on the matrix of the transverse FLAIR-weighted images. Subsequently, the CBV voxel intensity values were extracted voxel-wise from the overlaid VOIs and exported for statistical analysis. For histogram analysis, the following seven parameters were derived from the rCBV histograms: mean, standard deviation (SD), as well as the 10th (C10), 25th (C25), 50th (C50), 75th (C75), and 90th (C90) percentiles.

Statistical Analyses

Data analyses were performed using IBM SPSS Statistics® Version 24 (IBM, Armonk, NY, USA). To account for potential inter-individual variations of the brain, the CBV data were normalized to the NAWM values in each patient, resulting in normalized rCBV [16].

The Shapiro-Wilk test for normal distributions was applied for all variables. The Mann-Whitney U-test was used to compare rCBV values between gliomas with the wild type and mutation of IDH1/2 and with maintained ATRX and loss of expression. Comparisons were also made between intact alleles and chromosome 1p/19 LOH as well as between the methylated and unmethylated MGMT pro-

Table 1 Histogram parameters of relative cerebral blood volume in tumor grading according to WHO 2016-based integrated tumor grades and molecular profiles

Histopathological characteristics								
Histology	Astrocytoma		GBM	Astrocytoma		GBM	Oligodendroglioma	
WHO grade	II	III	IV	II	III	IV	II	III
Molecular characteristics								
IDH1/2	Mutation			Wild type			Mutation	
ATRX	Loss of expression			Expression			Expression	
LOH 1p/19q	No			No			Yes	
n	17 (17%)	8 (6%)	6 (6%)	6 (6%)	16 (16%)	24 (24%)	17 (17%)	6 (6%)
Mean	1.09 ± 0.30	1.21 ± 0.45	1.87 ± 1.12	2.72 ± 0.80	2.63 ± 1.57	2.55 ± 1.29	1.94 ± 0.55	2.20 ± 0.64
SD	0.90 ± 0.29	0.76 ± 0.31	1.07 ± 0.32	1.60 ± 0.76	1.44 ± 0.61	1.65 ± 0.79	1.31 ± 0.47	1.23 ± 0.54
C10	0.39 ± 0.25	0.55 ± 0.24	0.77 ± 1.01	1.30 ± 0.34	1.18 ± 0.96	0.90 ± 0.53	0.69 ± 0.33	0.95 ± 0.29
C25	0.56 ± 0.26	0.74 ± 0.31	1.15 ± 1.10	1.67 ± 0.39	1.61 ± 1.08	1.38 ± 0.80	1.08 ± 0.37	1.27 ± 0.32
C50	0.84 ± 0.29	1.04 ± 0.40	1.67 ± 1.17	2.37 ± 0.73	2.30 ± 1.53	2.20 ± 1.25	1.66 ± 0.50	1.93 ± 0.51
C75	1.25 ± 0.36	1.49 ± 0.56	2.40 ± 1.34	3.17 ± 0.99	3.23 ± 2.00	3.30 ± 1.80	2.41 ± 0.73	2.89 ± 0.91
C90	2.00 ± 0.52	2.12 ± 0.78	3.27 ± 1.59	5.07 ± 2.23	4.64 ± 2.51	4.80 ± 2.36	3.54 ± 1.11	3.75 ± 1.30
Histopathological characteristics								
Histology	Astrocytoma and GBM			Astrocytoma and GBM			Oligodendroglioma	
WHO grade	All			All			All	
Molecular characteristics								
IDH1/2	Mutation			Wild type			Mutation	
ATRX	Loss of expression			Expression			Expression	
LOH 1p/19q	No			No			Yes	
n	31 (31%)			46 (46%)			23 (23%)	
Mean	1.25 ± 0.49			2.60 ± 1.33			2.00 ± 0.57	
SD	0.89 ± 0.31			1.56 ± 0.71			1.29 ± 0.47	
C10	0.50 ± 0.44			1.06 ± 0.72			0.76 ± 0.33	
C25	0.71 ± 0.50			1.51 ± 0.88			1.13 ± 0.36	
C50	1.03 ± 0.59			2.26 ± 1.30			1.74 ± 0.51	
C75	1.50 ± 0.74			3.26 ± 1.77			2.54 ± 0.79	
C90	2.23 ± 0.91			4.78 ± 2.34			3.60 ± 1.14	

IDH isocitrate dehydrogenase 1/2 mutation status, *ATRX* alpha-thalassemia/mental retardation syndrome X-linked expression status, *LOH* chromosome 1p/19q loss of heterozygosity, *GBM* glioblastoma, *SD* standard deviation, C_n nth percentile, *rCBV* relative cerebral blood volume
rCBV metrics are dimensionless.

Table 2 Histogram parameters of relative cerebral blood volume in glioma stratified according to molecular characteristics

Histopathological characteristics								
Histology	All	All	All	All	All	All	IDH_{wt} AS and GBM	
WHO grade	All	All	All	All	All	All	All	
Molecular characteristics								
-	IDH mutation	IDH wild type	ATRX loss	ATRX expression	1p/19q LOH	1p/19qintact	MGMT meth.	MGMT unmeth.
n	55 (55%)	45 (45%)	30 (30%)	70 (70%)	22 (22%)	78 (78%)	17 (37%)	29 (63%)
Mean	1.60 ± 0.69	2.60 ± 1.33	1.25 ± 0.49	2.36 ± 1.12	2.03 ± 0.56	2.00 ± 1.26	3.23 ± 1.70	2.08 ± 0.57
SD	1.07 ± 0.44	1.56 ± 0.71	0.89 ± 0.31	1.45 ± 0.63	1.30 ± 0.46	1.26 ± 0.66	1.99 ± 0.73	1.20 ± 0.45
C10	0.62 ± 0.41	1.06 ± 0.72	0.50 ± 0.44	0.94 ± 0.61	0.77 ± 0.33	0.81 ± 0.67	1.25 ± 0.93	0.89 ± 0.43
C25	0.90 ± 0.49	1.51 ± 0.88	0.71 ± 0.50	1.36 ± 0.73	1.13 ± 0.36	1.16 ± 0.83	1.82 ± 1.16	1.25 ± 0.44
C50	1.35 ± 0.65	2.26 ± 1.30	1.03 ± 0.59	2.05 ± 1.07	1.74 ± 0.50	1.71 ± 1.20	2.81 ± 1.68	1.80 ± 0.56
C75	1.98 ± 0.92	3.26 ± 1.77	1.50 ± 0.74	2.97 ± 1.49	2.56 ± 0.77	2.47 ± 1.66	4.06 ± 2.24	2.57 ± 0.83
C90	2.86 ± 1.21	4.78 ± 2.34	2.23 ± 0.91	4.30 ± 2.02	3.64 ± 1.11	3.64 ± 2.24	5.99 ± 2.80	3.75 ± 1.19

IDH Isocitrate-dehydrogenase 1/2 mutation status, *ATRX* alpha-thalassemia/mental retardation syndrome X-linked expression status, *LOH* chromosome 1p/19q loss of heterozygosity, *MGMT* O6-methylguanine DNA methyltransferase, *SD* standard deviation, $C_n$nth percentile
rCBV metrics are dimensionless.

Table 3 Diagnostic performance of relative cerebral blood volume histogram parameters in grading glioma according to their 2016 CNS WHO-based molecular profile

	Mean	SD	C10	C25	C50	C75	C90
IDH_{mut} AS—IDH_{wt}GBM							
p value	**<0.001**	**<0.001**	**<0.001**	**<0.001**	**<0.001**	**<0.001**	***<0.001***
ROC AUC	0.916	0.818	0.819	0.864	0.882	0.904	*0.922*
Optimal cut-off value	1.45	1.25	0.35	0.95	1.05	1.45	*2.55*
Sensitivity (%)	91	30	97	73	97	100	*94*
Specificity (%)	81	96	50	89	54	65	*77*
Diagnostic accuracy (%)	86.4	74.6	76.3	79.7	81.4	84.7	*86.4*
IDHmut AS-OD1p/19q-LOH							
p value	**<0.001**	0.014	0.018	**0.001**	***<0.001***	**<0.001**	**<0.001**
ROC AUC	0.872	0.747	0.757	0.854	*0.885*	0.878	0.852
Optimal cut-off value	1.45	1.45	0.35	0.85	*1.25*	1.65	2.55
Sensitivity (%)	82	36	100	86	*86*	91	86
Specificity (%)	81	100	50	81	*81*	73	77
Diagnostic accuracy	81.3	70.8	72.9	81.3	*83.3*	81.3	81.3
IDHwt GBM-OD1p/19q-LOH							
p value	0.699	0.820	0.532	0.798	1.0	1.0	0.401
ROC AUC	0.619	0.595	0.629	0.597	0.597	0.594	0.643

$IDH_{mut}AS$ isocitrate-dehydrogenase 1/2-mutated astrocytoma, *IDH_{wt} GBM* isocitrate-dehydrogenase 1/2 wild type glioblastoma, *$OD_{1p/19q\text{-}LOH}$* oligodendroglioma with chromosome 1p/19q loss of heterozygosity, *SD* standard deviation, C_n n^{th} percentile, *ROC AUC* receiver operating characteristic curves area under the curve
Significant *p* values at $\alpha = 0.0083$ are highlighted in bold.
The results with the highest Youden index were defined as the optimal cut-off values.
The histogram parameters with the highest discriminatory power are highlighted in italics.
The diagnostic accuracy was calculated using a CART-based decision tree algorithm with 10-fold cross-validation.
rCBV metrics are dimensionless.

moter. The Shapiro-Wilk test showed non-normal distribution in all groups and the Levené test showed that there was also no variance homogeneity in all groups. Thus, one-way analysis of variance (ANOVA) on ranks (Kruskal-Wallis test) with a post-hoc Dunn-Bonferroni correction was used for comparison between integrated glioma grades of 2016 CNS WHO as well as between grouped integrated diagnoses of IDH_{mut} AS, IDH_{wt} GBM, and $OD_{1p/19q\text{-}LOH}$. Tests of the six a priori hypotheses were conducted using Bonferroni adjusted alpha levels of 0.0083 per test (0.05/6). A classification and regression tree (CART) algorithm [28] with 10-fold cross-validation was used to determine the di-

agnostic accuracy. Receiver operating characteristic (ROC) curves were generated for all significant rCBV histogram parameters to determine the area under the curve (AUC). The results with the highest Youden index were defined as the optimal cut-off values.

Results

The inter-rater agreement was excellent (ICC, 0.893; 95% CI, 0.872–0.924) for VOI delineation.

Table 1, 2 and 3 show the integrated histopathological and molecular findings according to the 2016 CNS WHO as well as the grouped findings based on their molecular profile and clinical outcome [2, 3, 5, 26]. Additionally, Table 1 shows the histogram parameters of rCBV values with their standard deviations of the integrated diagnoses of 2016 CNS WHO as well as for grouped IDH_{mut} AS, IDH_{wt} GBM, and $OD_{1p/19q\text{-}LOH}$. Regarding the molecular markers separately, the findings and corresponding rCBV results for IDH1/2 mutation, ATRX expression, chromosome 1p/19q LOH, and MGMT methylation status are shown in Table 2.

Relative Cerebral Blood Volume Values Among 2016 CNS WHO Glioma Grades

For separate 2016 CNS WHO-based tumor grades, there were no statistically significant differences in the histogram parameters of rCBV values between IDH_{mut} AS2, AS3 and GBM, between IDH_{wt} AS2, AS3 and GBM and between 1p/19q-confirmed OD2 and OD3. The results are illustrated in Supplementary Fig. 1. The figure includes all *p* values.

Relative Cerebral Blood Volume Values Among Integrated Glioma Groups

For the grouped comparisons based on the molecular profile and clinical outcome [2, 3, 5, 26], all histogram parameters of rCBV were significantly lower in IDH_{mut} AS than in $OD_{1p/19q\text{-}LOH}$ and IDH_{wt} GBM. There was no significant difference between rCBV among patients with $OD_{1p/19q\text{-}LOH}$ and IDH_{wt} GBM. The corresponding *p* values of the histogram parameters are presented in Table 3. The table includes the ROC AUC and the optimal cut-off values as well as sensitivity, specificity, and diagnostic accuracy. Fig. 3a illustrates the C90 of rCBV in glioma grading according to their molecular profile. Supplementary Fig. 3 shows the results of multivariate and cross-validated CART analysis for non-invasive glioma classification according to their integrated molecular profile.

Relative Cerebral Blood Volume Values Among Separate Molecular Characteristics

For individual molecular characteristics, all histogram parameters of rCBV were significantly lower in tumors with the IDH1/2 mutation than in those with the wild type of IDH1/2. They were also significantly lower in patients with ATRX loss than in those with maintained ATRX expression. There was no significant difference between rCBV among patients with chromosome 1p/19q LOH and intact alleles. In patients with primary IDH_{wt} GBM the SD of rCBV was significantly higher and C90 was significantly lower in patients with an unmethylated MGMT promoter than in those with methylated MGMT promoter. All corresponding *p* values of the histogram parameters are presented in Table 4. The table includes the ROC AUC, the optimal cut-off values as well as sensitivity, specificity, and diagnostic accuracy. Fig. 3b–d illustrates significant histogram parameters of rCBV in glioma grading according to IDH1/2 mutation, ATRX expression, and MGMT methylation status. Representative ROC curves for rCBV results are displayed in Fig. 4.

Discussion

The purpose of this study was to assess the diagnostic performance of DSC-MRI for in vivo molecular profiling of human glioma. According to the newly applied integrated molecular approach of the current 2016 CNS WHO, the 90th percentile of rCBV can best identify the IDH1/2 mutation and ATRX expression statuses. In the IDH_{wt} GBM group the SD and 90th percentile of rCBV may differentiate between methylated and unmethylated MGMT promoters. In CART analysis, rCBV predicted the molecular subgroup in 76.3% of astroglial tumors. The diagnostic performance was reduced to 48.1% by including $OD_{1p/19q\text{-}LOH}$ into the analysis.

All tumors were classified according to the current 2016 CNS WHO criteria [2]; however, several recent neuropathological studies have indicated a grading problem with the 2016 CNS WHO [2, 3, 25, 26]. Reuss et al. demonstrated that the group of astrocytomas harboring an IDH mutation "can be considered to define a molecular and clinical homogenous entity" [2] with "virtually identical [...] patient age and [...] overall survival" [3] between IDH_{mut} diffuse (AS2) and anaplastic (AS3) astrocytomas. Furthermore, most IDH wild type astrocytomas (IDH_{wt} AS2 and AS3) "represent underdiagnosed GBM" [2]. Additionally, for $OD_{1p/19q\text{-}LOH}$, the "WHO grade does not seem to substantially affect overall survival" in the IDH_{mut} cohort [26], and recent data suggest that telomerase reverse transcriptase (TERT) mutation status in oligodendroglioma (OD) is

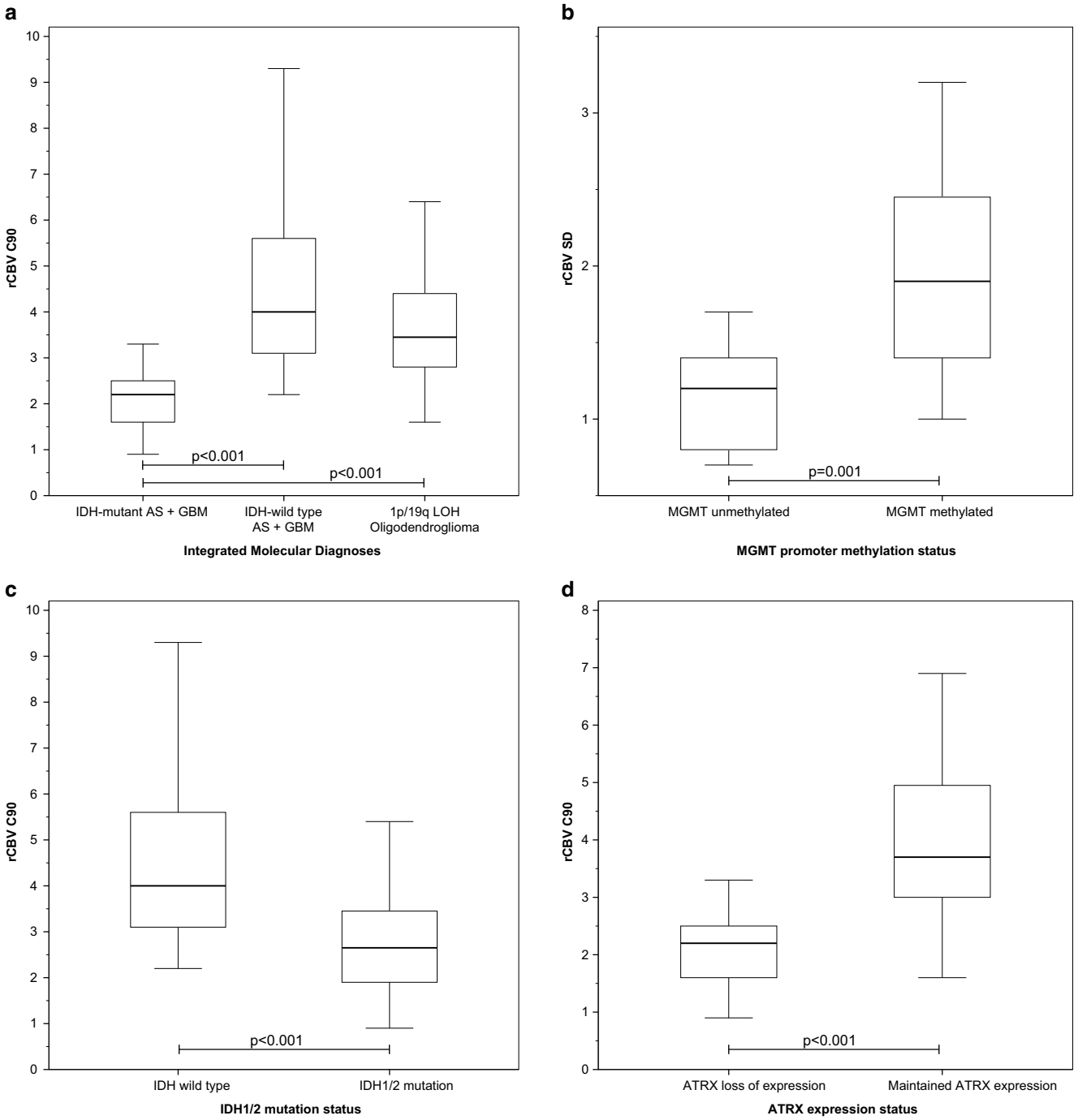

Fig. 3 Histogram parameters of normalized cerebral blood volume values in WHO 2016-based integrated tumor grading. Boxplots illustrate the 90th percentile of normalized cerebral blood volume (rCBV) values in glioma grading according to WHO-based histological findings (**a**), integrated molecular diagnoses of IDH mutant astrocytoma, 1p/19q-confirmed oligodendroglioma and IDH wild type glioblastoma (**b**), O6-methylguanine DNA methyltransferase (*MGMT*) promoter methylation status in primary IDH wild type glioblastoma, (**c**) isocitrate dehydrogenase (*IDH*) 1/2 mutation status, and (**d**) alpha-thalassemia/mental retardation syndrome X-linked (*ATRX*) expression. rCBV is dimensionless

Table 4 Diagnostic performance of relative cerebral blood volume histogram parameters in stratifying glioma according to their molecular characteristics

	Mean	SD	C10	C25	C50	C75	C90
IDH1/2 wild type–mutation							
p value	**<0.001**	**0.001**	**<0.001**	**<0.001**	**<0.001**	**<0.001**	***<0.001***
ROC AUC	0.780	0.716	0.732	0.755	0.752	0.762	*0.795*
Optimal cut-off value	1.45	1.25	1.05	0.95	2.30	3.30	*4.61*
Sensitivity (%)	52	77	90	67	87	85	*90*
Specificity (%)	91	61	46	73	42	46	*53*
Diagnostic accuracy (%)	67.9	70.4	71.6	70.4	70.4	70.4	*70.4*
ATRX maintained—loss of expression							
p value	**<0.001**	**<0.001**	**<0.001**	**<0.001**	**<0.001**	**<0.001**	***<0.001***
ROC AUC	0.898	0.798	0.794	0.860	0.884	0.894	*0.894*
Optimal cut-off value	1.45	1.25	0.35	0.85	1.05	1.45	*2.55*
Sensitivity (%)	87	92	98	82	96	96	*91*
Specificity (%)	81	45	50	77	62	66	*77*
Diagnostic accuracy (%)	85.2	76.5	82.7	80.2	85.2	86.4	*86.4*
Chromosome 1p/19q LOH—intact alleles							
p value	0.126	0.287	0.509	0.237	0.087	0.075	0.202
ROC AUC	0.611	0.577	0.548	0.586	0.624	0.629	0.592
MGMT methylated-unmethylated in all tumors							
p value	0.102	0.037	0.584	0.276	0.156	0.079	0.073
ROC AUC	0.607	0.636	0.536	0.571	0.593	0.615	0.617
MGMT methylated-unmethylated in IDH1/2 wild type gliomas							
p value	0.044	***0.001***	0.290	0.190	0.108	0.044	**0.007**
ROC AUC	0.706	*0.830*	0.611	0.637	0.665	0.706	0.769
Optimal cut-off value	3.0	*1.75*	1.35	1.90	2.65	3.87	4.05
Sensitivity (%)	53	*67*	40	47	53	53	73
Specificity (%)	94	*94*	89	89	94	89	78
Diagnostic accuracy (%)	75.8	*81.8*	66.7	69.7	75.8	72.2	75.8

$IDH_{mut}AS$ isocitrate dehydrogenase 1/2-mutated astrocytoma, *IDH_{wt} GBM* isocitrate dehydrogenase 1/2 wild type glioblastoma, *$OD_{1p/19q\text{-}LOH}$* oligodendroglioma with chromosome 1p/19q loss of heterozygosity, *SD* standard deviation, *C_n* n^{th} percentile, *ROC AUC* receiver operating characteristic curves area under the curve

Significant *p* values at $\alpha = 0.0083$ are highlighted in bold.

The results with the highest Youden index were defined as the optimal cut-off values.

The histogram parameters with the highest discriminatory power are highlighted in italics.

The diagnostic accuracy was calculated using a CART-based decision tree algorithm with 10-fold cross-validation.

rCBV metrics are dimensionless.

more prognostic than histological grading alone [6]. Therefore, IDH_{mut} AS2, IDH_{mut} AS3, and IDH_{mut} GBM were additionally grouped as IDH_{mut} AS; IDH_{wt} AS2, IDH_{wt} AS3, and IDH_{wt} GBM were classified as IDH_{wt} GBM; and OD2 and OD3 were grouped as $OD_{1p/19q\text{-}LOH}$ for statistical analysis based on their molecular profile and clinical outcome [2, 3, 5, 26].

The CBV reflects the vascular proliferation in central nervous system tumors [11, 12]. At the histopathological level, the increased microvascular proliferation has been shown to correlate with increased rCBV values [11, 13, 14]. The combination of ATRX loss and IDH1/2 mutations in the integrated approach characterizes diffuse astrocytoma (IDH_{mut} AS), including secondary GBM as its most aggressive histological subtype [25]. A GBM with the IDH1/2 mutation is described as a "homogeneous group" of GBM with a "lesser extent of necrosis" and "less frequent occurrence of vascular abnormalities" compared with the "heterogeneous presentation of more aggressive IDH1 wild-type" GBM, which show "more pronounced arcade-like vascular appearance" and a significantly higher contrast-enhancing component [29, 30]. Thus, lower rCBV values reflect the vascular features in IDH_{mut} AS, whereas primary IDH_{wt} GBM shows increased rCBV values because of increased microvascular proliferation [19]. Our rCBV values for IDH_{wt} GBM with maintained ATRX expression were significantly higher than for IDH_{mut} AS with ATRX loss, which corresponds to previously reported results [19]. Published values of rCBV for OD and oligoastrocytoma according to the 2007 CNS WHO were significantly higher than

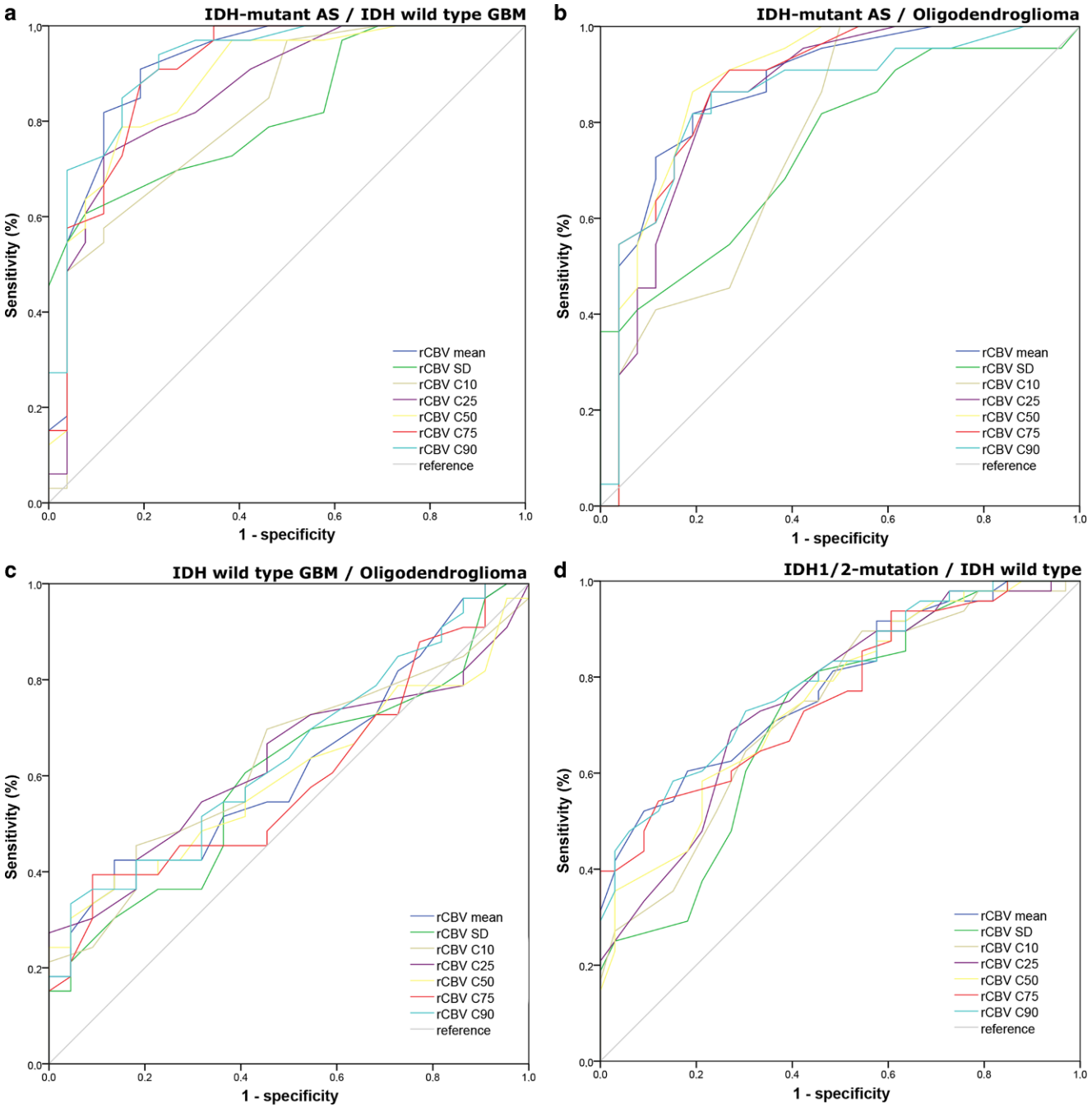

Fig. 4 Area under the receiver operating characteristics curves in WHO 2016-based tumor grading and integrated molecular approach. The AUC of ROC curves for discrimination between integrated molecular diagnoses of **a** IDH-mutant astrocytoma and IDH wild type glioblastoma, **b** IDH-mutant astrocytoma and 1p/19q-confirmed oligodendroglioma, **c** IDH-mutant astrocytoma and IDH wild type glioblastoma, as well as between molecular characteristics of **d** IDH1/2 mutation and IDH wild type, **e** maintained ATRX and loss of expression and **f** O6-methylguanine DNA methyltransferase (MGMT) promoter methylation status in primary IDH wild type glioblastoma, based on histogram parameters of rCBV values. *AUC* area under the curve, *ROC* receiver operating characteristics, *IDH* isocitrate-dehydrogenase, *ATRX* alpha-thalassemia/mental retardation syndrome X-linked expression, *MGMT* O6-methylguanine DNA methyltransferase, *rCBV* normalized cerebral blood volume, *GBM* glioblastoma, *SD* standard deviation

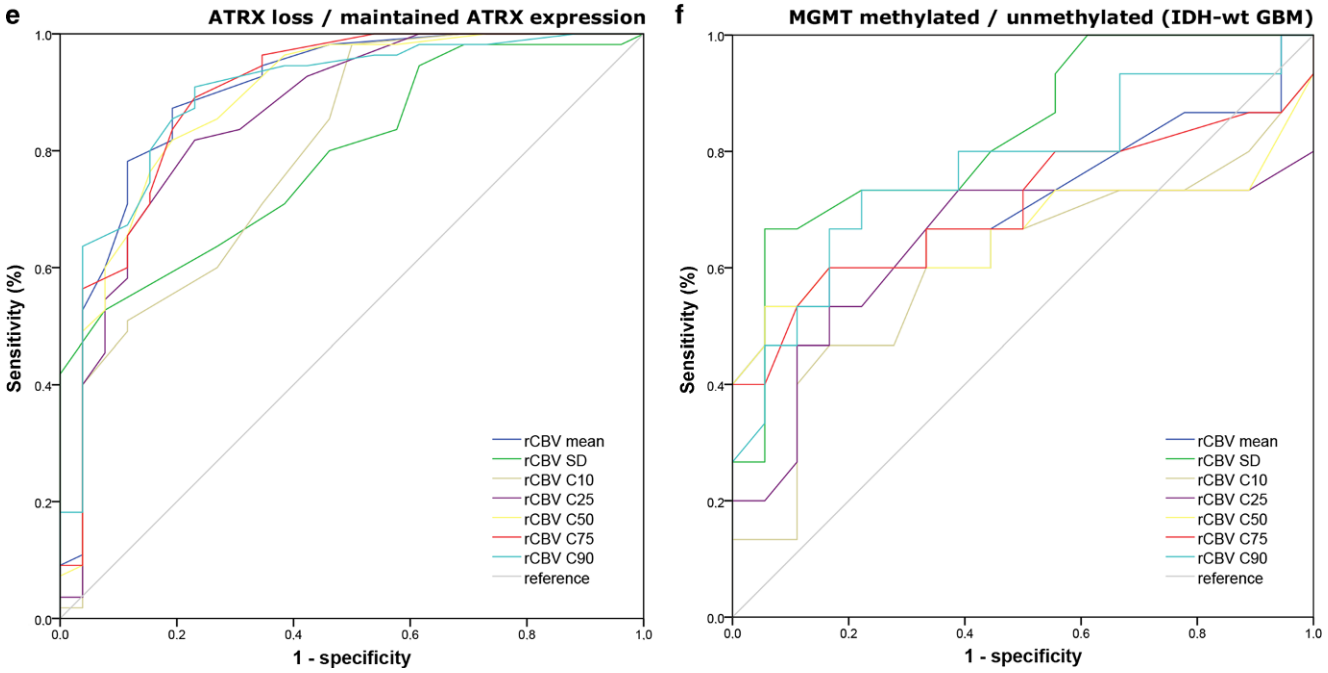

Fig. 4 (continued)

those for astrocytic tumors [16, 31]. Furthermore, oligodendroglial tumors with chromosome 1p/19q LOH were associated with significantly increased tumor perfusion, along with elevated rCBV values and epidermal growth factor receptor (EGFR) and vascular endothelial growth factor (VEGF) expression [32, 33]. The exact mechanism for elevated rCBV in oligodendroglial tumors remains unclear, but it may be associated with increased microvascular density [34], higher metabolic activity [32], distinct vascular pattern [15] or the degree and type of capillarization [16]. Our rCBV values of $OD_{1p/19q\text{-}LOH}$ were significantly higher than those of IDH_{mut} AS; however, they could not be significantly differentiated from those of IDH_{wt} GBM because of a substantial overlap of rCBV values. Using multivariate and cross-validated CART analysis (see Supplementary Fig. 3), rCBV correctly predicted the molecular subtype in three quarters of astrocytic gliomas. By including $OD_{1p/19q\text{-}LOH}$ into analysis, the diagnostic performance was substantially decreased to approximately 50%. Therefore, rCBV is not feasible as an independent biomarker for predicting chromosome 1p/19q LOH or for differentiating between the integrated molecular glioma subgroups of $OD_{1p/19q\text{-}LOH}$ and IDH_{wt} GBM.

We found contradictory reports for the individual 2016 CNS WHO tumor grades. Tan et al. [18] found significant differences of rCBV values between an IDH_{mut} and an IDH_{wt} cohort of each WHO grade, whereas Hilario et al. stated that "grade II and III tumors also did not differ when astrocytomas, oligodendrogliomas, and oligoastrocytomas were considered separately" [35]. We found no significant differences of rCBV values among AS2, AS3, and GBM both within the IDH_{mut} and the IDH_{wt} group, which supports the hypotheses of Reuss et al. [2, 3] and the findings of Hilario et al. [35]; however, we found a trend towards higher rCBV values in IDH_{mut} GBM than in IDH_{mut} AS2 and AS3 representing the degree of neovascularization. Additionally, for $OD_{1p/19q\text{-}LOH}$, we found similar rCBV values among OD2 and OD3, which is consistent with Suzuki et al. [26] and Hilario et al. [35].

In isolation, rCBV shows promise for predicting IDH1/2 mutation status and ATRX expression. These results are partly consistent with previously-published results by Lee et al. [36], who found significant differences in rCBV histogram parameters between patients with the wild type and IDH1/2 mutation in astrocytoma; however, that study was limited by excluding OD with synchronous IDH1/2 mutation and chromosome 1p/19q LOH, which can have significant overlap of rCBV values with GBM [15, 16]. Kickingereder et al. [19] found higher rCBV histogram parameter values in IDH_{wt} AS2, AS3, and GBM compared with IDH_{mut} AS2, AS3, and GBM or $OD_{1p/19q\text{-}LOH}$. They reported a diagnostic accuracy of 88% for predicting the IDH1/2 mutation. Our findings show similar accuracy when $OD_{1p/19q\text{-}LOH}$ is not included (Supplementary Table 1, Supplementary Fig. 2); however, taking $OD_{1p/19q\text{-}LOH}$ into account limits the role of rCBV in predicting IDH1/2 mutation status.

The ATRX has been shown to be a potential marker for prediction of IDH/H3F3A mutations and substratification of diffuse gliomas into survival relevant tumor groups [4]. Our rCBV values for gliomas with maintained ATRX expres-

sion, which is a typical feature of IDH_{wt} GBM, were significantly higher than those of gliomas with loss of ATRX expression, and the C90 of rCBV showed a diagnostic accuracy of 86.4% in predicting the ATRX expression status. We did not find any published corresponding rCBV values for individual comparison of ATRX expression status.

The MGMT can be regarded as an independent prognostic factor in patients with primary GBM [7] as MGMT promoter methylation increases responsiveness to temozolomide chemotherapy [24]. Ryoo et al. [37] found significantly higher rCBV values in GBMs with an unmethylated MGMT promoter than in those with a methylated MGMT; however, they did not take the IDH1/2 mutation status into account and analyzed only a small cohort of 25 patients. Conversely, our rCBV values were significantly higher in IDH_{wt} GBMs with a methylated MGMT than in those with an unmethylated MGMT. These findings support the hypotheses of Chahal et al. [38], who found that MGMT-positive cells displayed higher levels of vascular endothelial growth factor receptor 1 (VEGFR-1) compared with [MGMT unmethylated] U87/EV cells leading to higher vascularization of GBM. Our findings also support Kim et al. [39], who found that the "association between high CBF and a favorable 6-month outcome was more significant in the MGMT promoter methylation group" [39] in GBM but regardless of their molecular profile; however, further studies are needed to explore the role of DSC MRI in additional prognostic MGMT subgroups.

Limitations

This study is limited by potential selection bias because of the relatively small numbers of patients with IDH_{mut} GBM (secondary glioblastoma) and IDH_{wt} AS2 (early precursor lesion of IDH_{wt} GBM); however, these numbers represent their natural incidence [2, 3, 25, 26, 40]. Additionally, the process of VOI delineation may have been subject to sampling bias because glioma infiltration may extend beyond T2 signal abnormalities [41, 42]; however, studies have shown that the difference in tumor delimitation among different observers has a minor impact regarding the large number of voxels included in the histogram analysis [43, 44].

Conclusion

In the context of the revised 2016 CNS WHO, our findings support the upcoming integrated "morpho-molecular" approach towards characterization of glioma [2, 3, 26, 40]. As isolated factors, the C90 of rCBV from DSC-MRI shows the highest potential for predicting ATRX expression and IDH1/2 mutation status. Additionally, the SD and C90 of rCBV show promise for predicting the MGMT methylation profile of IDH_{wt} GBM. Considering the diagnostic and prognostic significance of these molecular markers, rCBV appears to be a promising in vivo biomarker for glioma; however, taking $OD_{1p/19q\text{-}LOH}$ into account limits the diagnostic potential of rCBV for non-invasively predicting the molecular glioma subtype due to substantial overlap between $OD_{1p/19q\text{-}LOH}$ and IDH_{wt} GBM. Thus, further studies using a multiparametric approach are needed to explore the role of DSC MRI as a prognostic biomarker in molecular glioma subgroups.

Funding JS was supported by the Else-Übelmesser Foundation (grant no. 30.19845). The funders had no role in study design, data collection and analysis, decision to publish, or preparation of the manuscript.

Conflict of interest J.-M. Hempel, J. Schittenhelm, U. Klose, B. Bender, G. Bier, M. Skardelly, G. Tabatabai, S. Castaneda Vega, U. Ernemann and C. Brendle declare that they have no competing interests.

References

1. Louis DN, Perry A, Reifenberger G, von Deimling A, Figarella-Branger D, Cavenee WK, Ohgaki H, Wiestler OD, Kleihues P, Ellison DW. The 2016 World Health Organization classification of tumors of the central nervous system: a summary. Acta Neuropathol. 2016;131:803–20.
2. Reuss DE, Kratz A, Sahm F, Capper D, Schrimpf D, Koelsche C, Hovestadt V, Bewerunge-Hudler M, Jones DT, Schittenhelm J, Mittelbronn M, Rushing E, Simon M, Westphal M, Unterberg A, Platten M, Paulus W, Reifenberger G, Tonn JC, Aldape K, Pfister SM, Korshunov A, Weller M, Herold-Mende C, Wick W, Brandner S, von Deimling A. Adult IDH wild type astrocytomas biologically and clinically resolve into other tumor entities. Acta Neuropathol. 2015;130:407–17.
3. Reuss DE, Mamatjan Y, Schrimpf D, Capper D, Hovestadt V, Kratz A, Sahm F, Koelsche C, Korshunov A, Olar A, Hartmann C, Reijneveld JC, Wesseling P, Unterberg A, Platten M, Wick W, Herold-Mende C, Aldape K, von Deimling A. IDH mutant diffuse and anaplastic astrocytomas have similar age at presentation and little difference in survival: a grading problem for WHO. Acta Neuropathol. 2015;129:867–73.
4. Ebrahimi A, Skardelly M, Bonzheim I, Ott I, Mühleisen H, Eckert F, Tabatabai G, Schittenhelm J. ATRX immunostaining predicts IDH and H3F3A status in gliomas. Acta Neuropathol Commun. 2016;4:60.
5. Pekmezci M, Rice T, Molinaro AM, Walsh KM, Decker PA, Hansen H, Sicotte H, Kollmeyer TM, McCoy LS, Sarkar G, Perry A, Giannini C, Tihan T, Berger MS, Wiemels JL, Bracci PM, Eckel-Passow JE, Lachance DH, Clarke J, Taylor JW, Luks T, Wiencke JK, Jenkins RB, Wrensch MR. Adult infiltrating gliomas with WHO 2016 integrated diagnosis: additional prognostic roles of ATRX and TERT//Adult infiltrating gliomas with WHO 2016 integrated diagnosis: Additional prognostic roles of ATRX and TERT. Acta Neuropathol. 2017;133:1001–16.
6. Abedalthagafi M, Phillips JJ, Kim GE, Mueller S, Haas-Kogen DA, Marshall RE, Croul SE, Santi MR, Cheng J, Zhou S, Sullivan LM, Martinez-Lage M, Judkins AR, Perry A. The alternative lengthening of telomere phenotype is significantly associated with loss of ATRX expression in high-grade pediatric and adult astrocytomas: a multi-institutional study of 214 astrocytomas. Mod Pathol. 2013;26:1425–32.

7. Hegi ME, Diserens AC, Gorlia T, Hamou MF, de Tribolet N, Weller M, Kros JM, Hainfellner JA, Mason W, Mariani L, Bromberg JE, Hau P, Mirimanoff RO, Cairncross JG, Janzer RC, Stupp R. MGMT gene silencing and benefit from temozolomide in glioblastoma. N Engl J Med. 2005;352:997–1003.
8. Stupp R, Mason WP, van den Bent MJ, Weller M, Fisher B, Taphoorn MJ, Belanger K, Brandes AA, Marosi C, Bogdahn U, Curschmann J, Janzer RC, Ludwin SK, Gorlia T, Allgeier A, Lacombe D, Cairncross JG, Eisenhauer E, Mirimanoff RO; European Organisation for Research and Treatment of Cancer Brain Tumor and Radiotherapy Groups; National Cancer Institute of Canada Clinical Trials Group. Radiotherapy plus concomitant and adjuvant temozolomide for glioblastoma. N Engl J Med. 2005;352:987–96.
9. van den Bent MJ, Baumert B, Erridge SC, Vogelbaum MA, Nowak AK, Sanson M, Brandes AA, Clement PM, Baurain JF, Mason WP, Wheeler H, Chinot OL, Gill S, Griffin M, Brachman DG, Taal W, Rudà R, Weller M, McBain C, Reijneveld J, Enting RH, Weber DC, Lesimple T, Clenton S, Gijtenbeek A, Pascoe S, Herrlinger U, Hau P, Dhermain F, van Heuvel I, Stupp R, Aldape K, Jenkins RB, Dubbink HJ, Dinjens WNM, Wesseling P, Nuyens S, Golfinopoulos V, Gorlia T, Wick W, Kros JM. Interim results from the CATNON trial (EORTC study 26053-22054) of treatment with concurrent and adjuvant temozolomide for 1p/19q non-co-deleted anaplastic glioma: a phase 3, randomised, open-label intergroup study. Lancet. 2017;390:1645–53.
10. Shiroishi MS, Castellazzi G, Boxerman JL, D'Amore F, Essig M, Nguyen TB, Provenzale JM, Enterline DS, Anzalone N, Dörfler A, Rovira À, Wintermark M, Law M. Principles of T2 *-weighted dynamic susceptibility contrast MRI technique in brain tumor imaging. J Magn Reson Imaging. 2015;41:296–313.
11. Aronen HJ, Gazit IE, Louis DN, Buchbinder BR, Pardo FS, Weisskoff RM, Harsh GR, Cosgrove GR, Halpern EF, Hochberg FH. Cerebral blood volume maps of gliomas: comparison with tumor grade and histologic findings. Radiology. 1994;191:41–51.
12. Sugahara T, Korogi Y, Kochi M, Ikushima I, Hirai T, Okuda T, Shigematsu Y, Liang L, Ge Y, Ushio Y, Takahashi M. Correlation of MR imaging-determined cerebral blood volume maps with histologic and angiographic determination of vascularity of gliomas. AJR Am J Roentgenol. 1998;171:1479–86.
13. Barajas RF Jr, Phillips JJ, Parvataneni R, Molinaro A, Essock-Burns E, Bourne G, Parsa AT, Aghi MK, McDermott MW, Berger MS, Cha S, Chang SM, Nelson SJ. Regional variation in histopathologic features of tumor specimens from treatment-naive glioblastoma correlates with anatomic and physiologic MR Imaging. Neuro-Oncology. 2012;14:942–54.
14. Server A, Graff BA, Orheim TE, Schellhorn T, Josefsen R, Gadmar ØB, Nakstad PH. Measurements of diagnostic examination performance and correlation analysis using microvascular leakage, cerebral blood volume, and blood flow derived from 3T dynamic susceptibility-weighted contrast-enhanced perfusion MR imaging in glial tumor grading. Neuroradiology. 2011;53:435–47.
15. Cha S, Tihan T, Crawford F, Fischbein NJ, Chang S, Bollen A, Nelson SJ, Prados M, Berger MS, Dillon WP. Differentiation of low-grade oligodendrogliomas from low-grade astrocytomas by using quantitative blood-volume measurements derived from dynamic susceptibility contrast-enhanced MR imaging. AJNR Am J Neuroradiol. 2005;26:266–73.
16. Lev MH, Ozsunar Y, Henson JW, Rasheed AA, Barest GD, Harsh GR 4th, Fitzek MM, Chiocca EA, Rabinov JD, Csavoy AN, Rosen BR, Hochberg FH, Schaefer PW, Gonzalez RG. Glial tumor grading and outcome prediction using dynamic spin-echo MR susceptibility mapping compared with conventional contrast-enhanced MR: confounding effect of elevated rCBV of oligodendrogliomas corrected. AJNR Am J Neuroradiol. 2004;25:214–21.
17. Sunwoo L, Choi SH, Yoo RE, Kang KM, Yun TJ, Kim TM, Lee SH, Park CK, Kim JH, Park SW, Sohn CH, Won JK, Park SH, Kim IH. Paradoxical perfusion metrics of high-grade gliomas with an oligodendroglioma component: quantitative analysis of dynamic susceptibility contrast perfusion MR imaging. Neuroradiology. 2015;57:1111–20.
18. Tan W, Xiong J, Huang W, Wu J, Zhan S, Geng D. Noninvasively detecting Isocitrate dehydrogenase 1 gene status in astrocytoma by dynamic susceptibility contrast MRI. J Magn Reson Imaging. 2017;45:492–9.
19. Kickingereder P, Sahm F, Radbruch A, Wick W, Heiland S, von Deimling A, Bendszus M, Wiestler B. IDH mutation status is associated with a distinct hypoxia/angiogenesis transcriptome signature which is non-invasively predictable with rCBV imaging in human glioma. Sci Rep. 2015;5:16238.
20. Capper D, Weissert S, Balss J, Habel A, Meyer J, Jäger D, Ackermann U, Tessmer C, Korshunov A, Zentgraf H, Hartmann C, von Deimling A. Characterization of R132H mutation-specific IDH1 antibody binding in brain tumors. Brain Pathol. 2010;20:245–54.
21. Schittenhelm J, Mittelbronn M, Meyermann R, Melms A, Tatagiba M, Capper D. Confirmation of R132H mutation of isocitrate dehydrogenase 1 as an independent prognostic factor in anaplastic astrocytoma. Acta Neuropathol. 2011;122:651–2.
22. Hartmann C, Meyer J, Balss J, Capper D, Mueller W, Christians A, Felsberg J, Wolter M, Mawrin C, Wick W, Weller M, Herold-Mende C, Unterberg A, Jeuken JW, Wesseling P, Reifenberger G, von Deimling A. Type and frequency of IDH1 and IDH2 mutations are related to astrocytic and oligodendroglial differentiation and age: a study of 1,010 diffuse gliomas. Acta Neuropathol. 2009;118:469–74.
23. Thon N, Eigenbrod S, Grasbon-Frodl EM, Ruiter M, Mehrkens JH, Kreth S, Tonn JC, Kretzschmar HA, Kreth FW. Novel molecular stereotactic biopsy procedures reveal intratumoral homogeneity of loss of heterozygosity of 1p/19q and TP53 mutations in World Health Organization grade II gliomas. J Neuropathol Exp Neurol. 2009;68:1219–28.
24. Gerson SL. MGMT: its role in cancer aetiology and cancer therapeutics. Nat Rev Cancer. 2004;4:296–307.
25. Reuss DE, Sahm F, Schrimpf D, Wiestler B, Capper D, Koelsche C, Schweizer L, Korshunov A, Jones DT, Hovestadt V, Mittelbronn M, Schittenhelm J, Herold-Mende C, Unterberg A, Platten M, Weller M, Wick W, Pfister SM, von Deimling A. ATRX and IDH1-R132H immunohistochemistry with subsequent copy number analysis and IDH sequencing as a basis for an "integrated" diagnostic approach for adult astrocytoma, oligodendroglioma and glioblastoma. Acta Neuropathol. 2015;129:133–46.
26. Suzuki H, Aoki K, Chiba K, Sato Y, Shiozawa Y, Shiraishi Y, Shimamura T, Niida A, Motomura K, Ohka F, Yamamoto T, Tanahashi K, Ranjit M, Wakabayashi T, Yoshizato T, Kataoka K, Yoshida K, Nagata Y, Sato-Otsubo A, Tanaka H, Sanada M, Kondo Y, Nakamura H, Mizoguchi M, Abe T, Muragaki Y, Watanabe R, Ito I, Miyano S, Natsume A, Ogawa S. Mutational landscape and clonal architecture in grade II and III gliomas. Nat Genet. 2015;47:458–68.
27. Tozer DJ, Jäger HR, Danchaivijitr N, Benton CE, Tofts PS, Rees JH, Waldman AD. Apparent diffusion coefficient histograms may predict low-grade glioma subtype. NMR Biomed. 2007;20:49–57.
28. Breiman L. Classification and regression trees. Boca Raton: Chapman & Hall/CRC; 1984.
29. Popov S, Jury A, Laxton R, Doey L, Kandasamy N, Al-Sarraj S, Jürgensmeier JM, Jones C. IDH1-associated primary glioblastoma in young adults displays differential patterns of tumour and vascular morphology. PLoS One. 2013;8:e56328.
30. Lai A, Kharbanda S, Pope WB, Tran A, Solis OE, Peale F, Forrest WF, Pujara K, Carrillo JA, Pandita A, Ellingson BM, Bowers CW, Soriano RH, Schmidt NO, Mohan S, Yong WH, Seshagiri S, Modrusan Z, Jiang Z, Aldape KD, Mischel PS, Liau LM, Escovedo CJ, Chen W, Nghiemphu PL, James CD, Prados MD, Westphal

M, Lamszus K, Cloughesy T, Phillips HS. Evidence for sequenced molecular evolution of IDH1 mutant glioblastoma from a distinct cell of origin. J Clin Oncol. 2011;29:4482–90.
31. Saito T, Yamasaki F, Kajiwara Y, Abe N, Akiyama Y, Kakuda T, Takeshima Y, Sugiyama K, Okada Y, Kurisu K. Role of perfusion-weighted imaging at 3T in the histopathological differentiation between astrocytic and oligodendroglial tumors. Eur J Radiol. 2012;81:1863–9.
32. Whitmore RG, Krejza J, Kapoor GS, Huse J, Woo JH, Bloom S, Lopinto J, Wolf RL, Judy K, Rosenfeld MR, Biegel JA, Melhem ER, O'Rourke DM. Prediction of oligodendroglial tumor subtype and grade using perfusion weighted magnetic resonance imaging. J Neurosurg. 2007;107:600–9.
33. Kapoor GS, Gocke TA, Chawla S, Whitmore RG, Nabavizadeh A, Krejza J, Lopinto J, Plaum J, Maloney-Wilensky E, Poptani H, Melhem ER, Judy KD, O'Rourke DM. Magnetic resonance perfusion-weighted imaging defines angiogenic subtypes of oligodendroglioma according to 1p19q and EGFR status. J Neurooncol. 2009;92:373–86.
34. Chan AS, Leung SY, Wong MP, Yuen ST, Cheung N, Fan YW, Chung LP. Expression of vascular endothelial growth factor and its receptors in the anaplastic progression of astrocytoma, oligodendroglioma, and ependymoma. Am J Surg Pathol. 1998;22:816–26.
35. Hilario A, Ramos A, Perez-Nuñez A, Salvador E, Millan JM, Lagares A, Sepulveda JM, Gonzalez-Leon P, Hernandez-Lain A, Ricoy JR. The added value of apparent diffusion coefficient to cerebral blood volume in the preoperative grading of diffuse gliomas. AJNR Am J Neuroradiol. 2012;33:701–7.
36. Lee S, Choi SH, Ryoo I, Yoon TJ, Kim TM, Lee SH, Park CK, Kim JH, Sohn CH, Park SH, Kim IH. Evaluation of the microenvironmental heterogeneity in high-grade gliomas with IDH1/2 gene mutation using histogram analysis of diffusion-weighted imaging and dynamic-susceptibility contrast perfusion imaging. J Neurooncol. 2015;121:141–50.
37. Ryoo I, Choi SH, Kim JH, Sohn CH, Kim SC, Shin HS, Yeom JA, Jung SC, Lee AL, Yun TJ, Park CK, Park SH. Cerebral blood volume calculated by dynamic susceptibility contrast-enhanced perfusion MR imaging: Preliminary correlation study with glioblastoma genetic profiles. PLoS One. 2013;8:e71704.
38. Chahal M, Xu Y, Lesniak D, Graham K, Famulski K, Christensen JG, Aghi M, Jacques A, Murray D, Sabri S, Abdulkarim B. MGMT modulates glioblastoma angiogenesis and response to the tyrosine kinase inhibitor sunitinib. Neuro-Oncology. 2010;12:822–33.
39. Kim C, Kim HS, Shim WH, Choi CG, Kim SJ, Kim JH. Recurrent Glioblastoma: combination of high cerebral blood flow with MGMT promoter methylation is associated with benefit from low-dose temozolomide rechallenge at first recurrence. Radiology. 2017;282:212–21.
40. Unruh D, Schwarze SR, Khoury L, Thomas C, Wu M, Chen L, Chen R, Liu Y, Schwartz MA, Amidei C, Kumthekar P, Benjamin CG, Song K, Dawson C, Rispoli JM, Fatterpekar G, Golfinos JG, Kondziolka D, Karajannis M, Pacione D, Zagzag D, McIntyre T, Snuderl M, Horbinski C. Mutant IDH1 and thrombosis in gliomas. Acta Neuropathol. 2016;132:917–30.
41. Price SJ, Jena R, Burnet NG, Hutchinson PJ, Dean AF, Peña A, Pickard JD, Carpenter TA, Gillard JH. Improved delineation of glioma margins and regions of infiltration with the use of diffusion tensor imaging: an image-guided biopsy study. AJNR Am J Neuroradiol. 2006;27:1969–74.
42. Grier JT, Batchelor T. Low-grade gliomas in adults. Oncologist. 2006;11:681–93.
43. Emblem KE, Nedregaard B, Nome T, Due-Tonnessen P, Hald JK, Scheie D, Borota OC, Cvancarova M, Bjornerud A. Glioma grading by using histogram analysis of blood volume heterogeneity from MR-derived cerebral blood volume maps. Radiology. 2008;247:808–17.
44. Kim H, Choi SH, Kim JH, Ryoo I, Kim SC, Yeom JA, Shin H, Jung SC, Lee AL, Yun TJ, Park CK, Sohn CH, Park SH. Gliomas: application of cumulative histogram analysis of normalized cerebral blood volume on 3T MRI to tumor grading. PLoS One. 2013;8:e63462.

Affiliations

Johann-Martin Hempel[1] · Jens Schittenhelm[2] · Uwe Klose[1] · Benjamin Bender[1] · Georg Bier[1] · Marco Skardelly[3] · Ghazaleh Tabatabai[4] · Salvador Castaneda Vega[5] · Ulrike Ernemann[1] · Cornelia Brendle[1]

[1] Department of Neuroradiology, Eberhard Karls University, Hoppe-Seyler-Str. 3, 72076 Tübingen, Germany

[2] Institute of Neuropathology, Eberhard Karls University, Tübingen, Germany

[3] Department of Neurosurgery, Eberhard Karls University, Tübingen, Germany

[4] Centre of Neurooncology, Comprehensive Cancer Center Tübingen-Stuttgart, Eberhard Karls University, Tübingen, Germany

[5] Werner Siemens Imaging Center, Department of Preclinical Imaging and Radiopharmacy, Eberhard Karls University, Tübingen, Germany